BMJ Open

Can microstructural MRI detect subclinical tissue injury in subjects with asymptomatic cervical spinal cord compression? A prospective cohort study

Allan R Martin,[1] Benjamin De Leener,[2] Julien Cohen-Adad,[2] David W Cadotte,[3] Aria Nouri,[1] Jefferson R Wilson,[1] Lindsay Tetreault,[1,4] Adrian P Crawley,[5] David J Mikulis,[5] Howard Ginsberg,[5] Michael G Fehlings[1]

To cite: Martin AR, De Leener B, Cohen-Adad J, *et al*. Can microstructural MRI detect subclinical tissue injury in subjects with asymptomatic cervical spinal cord compression? A prospective cohort study. *BMJ Open* 2018;**8**:e019809. doi:10.1136/bmjopen-2017-019809

► Prepublication history and additional material for this paper are available online. To view these files, please visit the journal online (http://dx.doi.org/10.1136/bmjopen-2017-019809).

Received 27 March 2017
Revised 4 January 2018
Accepted 18 January 2018

[1]Division of Neurosurgery, Department of Surgery, University of Toronto, Toronto, Ontario, Canada
[2]Institute of Biomedical Engineering, École Polytechnique de Montréal, Montréal, Québec, Canada
[3]Department of Neurosurgery, University of Calgary, Calgary, Alberta, Canada
[4]Department of Medicine, University College Cork, Cork, Ireland
[5]Department of Medical Imaging, University of Toronto, Toronto, Ontario, Canada

Correspondence to
Dr Michael G Fehlings;
michael.fehlings@uhn.on.ca

ABSTRACT

Objectives Degenerative cervical myelopathy (DCM) involves extrinsic spinal cord compression causing tissue injury and neurological dysfunction. Asymptomatic spinal cord compression (ASCC) is more common, but its significance is poorly defined. This study investigates if: (1) ASCC can be automatically diagnosed using spinal cord shape analysis; (2) multiparametric quantitative MRI can detect similar spinal cord tissue injury as previously observed in DCM.

Design Prospective observational longitudinal cohort study.

Setting Single centre, tertiary care and research institution.

Participants 40 neurologically intact subjects (19 female, 21 male) divided into groups with and without ASCC.

Interventions None.

Outcome measures Clinical assessments: modified Japanese Orthopaedic Association score and physical examination. 3T MRI assessments: automated morphometric analysis compared with consensus ratings of spinal cord compression, and measures of tissue injury: cross-sectional area, diffusion fractional anisotropy, magnetisation transfer ratio and T2*-weighted imaging white to grey matter signal intensity ratio (T2*WI WM/GM) extracted from rostral (C1–3), caudal (C6–7) and maximally compressed levels.

Results ASCC was present in 20/40 subjects. Diagnosis with automated shape analysis showed area under the curve >97%. Five MRI metrics showed differences suggestive of tissue injury in ASCC compared with uncompressed subjects ($p<0.05$), while a composite of all 10 measures (average of z scores) showed highly significant differences ($p=0.002$). At follow-up (median 21 months), two ASCC subjects developed DCM.

Conclusions ASCC appears to be common and can be accurately and objectively diagnosed with automated morphometric analysis. Quantitative MRI appears to detect subclinical tissue injury in ASCC prior to the onset of neurological symptoms and signs. These findings require further validation, but offer the intriguing possibility of presymptomatic diagnosis and treatment of DCM and other spinal pathologies.

Strengths and limitations of this study

- ► The development of novel spinal cord shape analysis to objectively define and detect subtle spinal cord compression.
- ► Use of cutting-edge MRI techniques that are suitable for clinical translation to detect presymptomatic spinal cord tissue injury.
- ► Multiple measures of tissue injury that cross-validate each other and can be combined as a composite to increase statistical power.
- ► Lack of histopathological correlation data to confirm the presence of tissue injury.
- ► Modest sample size makes it difficult to draw conclusions about the clinical relevance of asymptomatic cord compression because the rate of progression to symptomatic myelopathy is not well defined.

INTRODUCTION

Degenerative cervical myelopathy (DCM) involves age-related degeneration of the discs, ligaments and vertebrae leading to extrinsic spinal cord compression and neurological dysfunction.[1] The prevalence of DCM is difficult to estimate, but it has been suggested that it is probably the most common cause of spinal cord dysfunction.[1 2] However, asymptomatic spinal cord compression (ASCC) is far more frequent, with prevalence estimates ranging from 8% to 59%.[3–8] Furthermore, spinal cord compression may be underestimated using supine MRI, which misses dynamic compression that is visible with flexion/extension MRI.[9] ASCC has received

little research attention, but one study found that it confers an increased risk of myelopathy development.[10]

Emerging quantitative MRI techniques offer in vivo measurement of spinal cord microstructural features and tissue injury.[11–13] Cross-sectional area (CSA) measures spinal cord compression and atrophy, the diffusion tensor imaging (DTI) metric fractional anisotropy (FA) measures axonal integrity, magnetisation transfer ratio (MTR) reflects myelin quantity and T2*-weighted imaging (T2*WI) white matter to grey matter signal intensity ratio (T2*WI WM/GM) is a novel biomarker that we recently introduced that correlates with demyelination, gliosis, calcium and iron concentrations.[12 14 15] These measures hold potential for earlier diagnosis of various conditions, but results to date have been modest and insufficient to drive clinical adoption.[11 13]

Our group previously reported a clinically feasible multiparametric MRI protocol that measures CSA, FA, MTR and T2*WI WM/GM across the cervical spinal cord.[14 15] In patients with DCM, these metrics reveal macrostructural and microstructural changes at the maximally compressed level (MCL) and in the uncompressed spinal cord above and below; significant clinical correlations and group differences compared with healthy subjects were found at rostral, MCL and caudal levels for FA and T2*WI WM/GM, while CSA and MTR showed significant results at rostral and MCL levels.[15] In the current study, we establish an objective definition of spinal cord compression and assess a newly developed automated spinal cord shape analysis for diagnostic accuracy. We test the hypothesis that subjects with ASCC experience tissue injury compared with uncompressed subjects, based on the same 10 MRI measures. Finally, we investigate the rate of symptomatic myelopathy development at follow-up.

METHODS

Study design and subjects

This study involved a secondary analysis of prospectively collected data that has been previously reported.[14 15] Forty-two subjects were recruited between October 2014 and December 2016 by convenience sampling and provided written informed consent. All clinical data collection and physical examinations were performed by a physician member of the UHN Spine Program. Subjects were examined to rule out neurological symptoms (numbness, weakness, fine motor dysfunction, gait/balance difficulties, urinary urgency/incontinence) and signs (hyper-reflexia, weakness, sensory deficits, Romberg sign, gait ataxia). Neck pain was not considered a neurological symptom. Subjects were also required to have 18/18 on the modified Japanese Orthopaedic Association (mJOA) score. Two subjects were excluded during screening; one showed gait ataxia and both had sensory deficits, hyper-reflexia and MRI evidence of spinal cord compression consistent with DCM. Follow-up assessments were performed by telephone, including mJOA administration. Subjects that reported any neurological symptoms underwent a complete neurological examination in person.

MRI acquisitions

Subjects underwent T2-weighted imaging (T2WI), DTI, magnetisation transfer (MT) and T2*WI at 3T (GE Signa Excite HDxt) covering C1–C7, as previously described.[14] DTI, MT and T2*WI images were acquired with 13 axial slices from C1 to C7. T2WI was performed with a fast imaging employing steady-state acquisition cycled phases sequence with 0.8×0.8×0.8 mm^3 isotropic resolution. DTI used spin echo single-shot echo planar imaging with three acquisitions averaged offline, b=800 s/mm^2 in 25 directions, five images with b=0 s/mm^2 and resolution of 1.25×1.25×5 mm^3. MT used 2D spoiled gradient echo ±MT prepulse, with 1×1×5 mm^3 voxels. T2*WI acquisition used multiecho recombined gradient echo with 3 echoes at 5, 10, 15 ms and resolution 0.6×0.6×4 mm^3. Total imaging time was 30–35 min including patient positioning, slice prescription and second order localised shimming (prior to DTI).

Image analysis

Images were inspected and excluded from analysis if image quality was poor or artefacts were present. Quantitative imaging data were analysed using Spinal Cord Toolbox (SCT) V.3.0,[16] including spinal cord segmentation, registration to the probabilistic SCT template and extraction of metrics with partial volume correction, as previously described.[14 15] Segmentations and registered images were reviewed, and if necessary segmentations were manually edited to correct inaccuracies.

Diagnosis of spinal cord compression followed a three-step process. First, anatomical images (T2WI and T2*WI) were independently examined by two raters (ARM, AN) for indentation, flattening, torsion or circumferential compression from extrinsic tissues (disc, ligament or bone), and the MCL was subjectively determined. Discrepancies were resolved by consensus. Effacement of the cerebrospinal fluid (CSF) was not considered compression. Second, automated shape analysis was performed on each axial section of the T2*WI spinal cord segmentation mask. 2D principal component analysis (PCA) identified the long and short axes, representing transverse and anterior–posterior (AP) directions, respectively (figure 1). Flattening was measured with compression ratio (CR)=AP/transverse diameter.[17] Indentation was measured using solidity=the percentage of area representing spinal cord within the convex hull that subtends the spinal cord. Torsion was measured with relative rotation, which was calculated as the angle between the transverse axis and horizontal, relative to adjacent slices (difference from the average rotation of above and below slices). Circumferential compression was not specifically measured with a shape metric, as it typically coincides with flattening. Receiver operating characteristic (ROC) curves were plotted to determine diagnostic accuracy of shape metrics at each intervertebral level compared

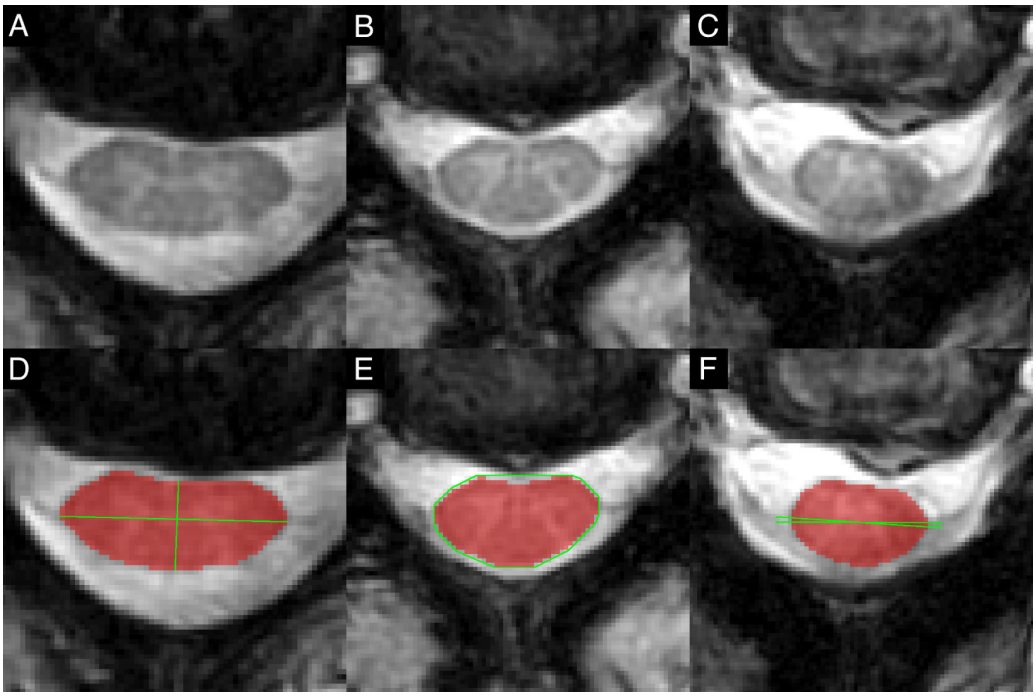

Figure 1 Automatic shape analysis. T2*WI of asymptomatic subjects showing flattening (A), indentation (B) and torsion (C) of the spinal cord. (D) The spinal cord segmentation (red) is analysed with 2D PCA to identify the long (transverse) and short (AP) axes (green) that intersect at the centre of mass, and CR is calculated as ratio of AP to transverse diameters to measure flattening. (E) A convex hull (green) is computed that surrounds the segmentation (red), and solidity is calculated as the ratio of segmented area to subtended area. (F) The angle between the transverse axis and horizontal is computed, and then relative rotation is calculated as the ratio between the current slice and average angle in slices above and below. AP, anterior–posterior; CR, compression ratio; PCA, principal component analysis; T2*WI, T2*-weighted imaging.

with consensus ratings. 95% CIs for area under the curve (AUC) were calculated using the DeLong method with 2000 stratified bootstrap replicates. Third, discrepancies between consensus ratings and shape analysis were discussed and diagnoses were revised by consensus if necessary. The mean and SD of shape parameters were calculated in uncompressed subjects for each rostrocaudal level. Analysis of variance (ANOVA) and Levene's test assessed if these values varied across rostrocaudal levels, in which case they were reported separately, and otherwise pooled mean, SD and diagnostic thresholds were calculated. Optimal diagnostic thresholds were then found by maximising Youden's Index.

Tissue injury was measured with CSA of the spinal cord, and FA, MTR and T2*WI WM/GM extracted from WM. Metrics were normalised for rostrocaudal level and averaged across rostral (C1–3), middle (C4–5 in uncompressed subjects or MCL, in ASCC subjects) and caudal (C6–7) levels. The MCL for subjects with multilevel compression was determined by consensus ratings after considering automated shape results. For MCL measurements, data from a single level were used for CSA, whereas three slices centred at MCL were averaged for FA, MTR and T2*WI WM/GM. Non-CSA metrics were also extracted from the ventral columns, lateral columns, dorsal columns and GM averaged across C1–C7 to identify focal injury. Metrics were normalised for age, sex, height, weight and cervical cord length, similar to our previous approach,[14] based on multiple linear regression with backward stepwise variable selection. However, the presence of spinal cord compression was included to measure independent effects of other variables, and age correction was performed (regardless of significance) to mitigate group differences. Ratios of MCL/rostral metrics were also calculated.[18]

Statistical analysis

Statistical analysis was performed with R V.3.3. Numerical data were summarised by mean±SD. Binary variables were compared using Fisher's exact test and numerical demographic variables were compared using two-tailed Welch's t-test. 95% CIs for frequencies were calculated using the Wilson procedure with continuity correction. MRI metrics were assumed to be normally distributed in subjects without spinal cord compression, whereas these data were assumed to be non-normal in ASCC subjects based on the hypothesis that they experience varying degrees of tissue injury. Results for individual ASCC subjects were analysed in terms of z scores (compared with the uncompressed population), whereas group differences between ASCC and uncompressed subjects were analysed with two-tailed Wilcoxon (non-parametric) test. The z scores of all 10 MRI metrics (using negative values for T2*WI WM/GM) were also averaged to yield a composite score, which was assumed to follow a t-distribution with 10 df (t_{10}) in uncompressed subjects, and results for individual

Table 1 Subject characteristics

Characteristic	Uncompressed subjects (n=20)	Compressed subjects (n=20)	P values
Age	39.4±12.8	54.9±13.8	0.0007*
Sex (male:female)	10:10	11:9	1.0
Height (cm)	172.7±9.4	170.5±8.0	0.43
Weight (kg)	71.1±10.4	79.8±13.3	0.03*
Neck length (mm)	106.3±9.6	107.0±9.4	0.81

Demographics and clinical measures are tabulated for subjects with and without cervical spinal cord compression.
*Significant differences (p<0.05) between groups.

subjects were analysed using t scores. A two-tailed binomial test compared the pattern of differences (increases or decreases) in ASCC versus uncompressed subjects with the pattern previously observed in DCM versus healthy subjects.[15] Logistic regression with backward stepwise elimination was used to develop a model for detecting tissue injury, retaining a maximum of four MRI metrics as independent variables. Significance was set at p<0.05 without correction for multiplicity due to the exploratory nature of this study, including individual measurements of $|z|>1.96$, $|t_{10}|>2.23$, and $|t_9|>2.26$.

RESULTS

Subject characteristics

Subject characteristics are listed in table 1. Individuals with ASCC were older (54.9 vs 39.4, p=0.0007) and weighed more (79.8 vs 71.1, p=0.03) than subjects without cord compression, while other characteristics (sex, height and neck length) did not differ.

Diagnosis of spinal cord compression

Consensus ratings identified 19 subjects with spinal cord compression at 41 levels (flattening: 20 levels, indentation: 30 levels, torsion: 8 levels, circumferential compression: 1 level). Relative to these ratings, automated shape analysis demonstrated an average AUC=99.2% (95% CI 97.3% to 100%) for flattening, pooled AUC=96.8% (95% CI 94.6% to 99.1%) for indentation and pooled AUC=99.2% (95% CI 98.0% to 100%) for torsion (table 2, figure 2). After reviewing shape analysis results, 3 levels were reclassified as flattened (total: 23 levels) and 1 level as indented (total: 31 levels). Remaining discrepancies were mostly at adjacent levels, which showed a transition between normal and abnormal shape. ANOVA detected that CR differed across rostrocaudal levels in uncompressed subjects (range: 58.7% to 67.2%), whereas solidity and relative rotation were invariant, yielding pooled normative values of 96.52%±0.56% and 0.3±1.5 degrees, respectively.

Final diagnostic ratings identified ASCC in 20/40 subjects (50%, 95% CI 34.1% to 65.9%). Six additional subjects (15%) without compression had effacement of the CSF. The frequency of ASCC increased with age (figure 3), including 15/21 (71.4%, 95% CI 47.7% to 87.8%) among subjects aged ≥50.

Details of spinal cord compression and shape metrics for each of the 20 ASCC subjects are provided online in supplementary table 1. Compression was primarily anterior at all compressed levels, related to disc±osteophyte complexes, with an element of posterior compression due to ligamentum flavum hypertrophy at nine levels. T2WI hyperintensity was not present in any subject, although one had a prominent central canal (1 mm diameter, within normal limits).

Variation of MRI metrics with age and other characteristics

CSA varied with cervical cord length and MTR varied with height at rostral and MCL levels, independent of the effect of cord compression (online supplementary table 2). None of the metrics varied significantly with age.

Quantitative MRI measures of tissue injury

Of 10, eight age-corrected MRI metrics showed the same direction of differences in ASCC versus uncompressed subjects as previously seen in DCM versus healthy subjects (p=0.11), including significant differences in five metrics: increased T2*WI WM/GM at all levels (rostral: p=0.03, MCL: p=0.005, caudal: p=0.01), decreased MCL FA (p=0.04) and decreased rostral MTR (p=0.046) (table 3). In contrast, CSA measures varied in the opposite direction from DCM, including significantly higher rostral CSA in ASCC (p=0.02). Ratios of MCL:rostral MRI metrics showed trends towards decreased FA ratio (p=0.06) and CSA ratio (p=0.09) in ASCC subjects (table 4).

Multivariate results

The MRI composite score showed greater differences than single metrics (p=0.002; table 3), including abnormal results (t_{10} score ≤2.23) in 6/20 compressed subjects (figure 4). When rostral and MCL CSA measures were replaced with CSA ratio, a revised composite score showed even stronger results ($p=8\times10^{-5}$), including 9/20 compressed subjects with abnormal results (t_9 score ≤2.26; figure 4). A logistic regression model retaining MCL T2*WI WM/GM (p=0.006), FA ratio (p=0.06), CSA ratio (p=0.11) and rostral MTR (p=0.34) yielded discrimination of 0.941 between compressed and uncompressed subjects ($p=2\times10^{-5}$).

Tissue injury by anatomical structure

Compressed subjects had decreased FA and MTR in the ventral columns (p=0.01, 0.02, respectively), while the

Table 2 Shape metrics

Shape parameter	Statistic	C2–3	C3–4	C4–5	C5–6	C6–7	Pooled values
CR (%)	Normal mean±SD	67.2±6.4	62.6±5.1	59.3±4.5	59.2±4.2	58.7±4.5	–
	Flattened frequency	0/40	3/40	5/40	7/40	5/40	20/200
	AUC	–	1.00	0.989	1.0	0.977	0.992
	Diagnostic threshold	–	53.1	52.0	49.9	50.5	–
	Sensitivity		100%	97.1%	100%	97.1%	–
	Specificity		100%	100%	100%	100%	–
Solidity (%)	Normal mean±SD	96.52±0.47	96.25±0.53	96.74±0.59	96.64±0.46	96.45±0.76	96.52±0.56
	Indented frequency	0/40	6/40	11/40	9/40	4/40	30/200
	AUC	–	0.976	0.984	0.979	1.0	0.968
	Diagnostic threshold	–	–	–	–	–	95.6
	Sensitivity	–	–	–	–	–	88.5%
	Specificity	–	–	–	–	–	96.7%
Relative rotation (degrees)	Normal mean±SD	0.0±1.3	0.5±1.6	0.5±1.3	0.4±1.4	0.3±1.5	0.3±1.5
	Rotated frequency	0/40	1/40	1/40	3/40	3/40	8/200
	AUC	–	1.0	1.0	1.0	0.991	0.992
	Diagnostic threshold	–	–	–	–	–	3.3
	Sensitivity						97.4%
	Specificity						100%

Data for CR, solidity and relative rotation are displayed for each intervertebral level from C2 to C7. Normal data are derived from 20 subjects with no cord compression and reported as mean±SD. Diagnostic accuracy is reported as AUC relative to consensus ratings (prior to revised diagnoses incorporating these results).
AUC, area under the curve; CR, compression ratio.

lateral columns, dorsal columns and grey matter did not show significant differences in these metrics (figure 5). In contrast, T2*WI WM/GM was increased in the lateral and dorsal columns (p=0.009, 0.0004, respectively) in compressed subjects, while the ventral columns showed no difference.

Clinical follow-up

All 20 ASCC subjects had follow-up assessments (median: 21 months, range: 3–27 months). Four subjects reported concerning new symptoms, and following physical examination two were diagnosed with DCM (10%, 95% CI 1.8% to 33.1%) and referred for surgical consultation. One experienced neck pain, intermittent right hand numbness and gait imbalance (mJOA=17), and examination showed marked gait ataxia, asymmetric hyper-reflexia and positive left Hoffman sign. The other had neck pain, left hand numbness and mild gait instability (mJOA=16), and examination revealed symmetric hyper-reflexia and mild gait ataxia. This individual sought medical attention with her family physician, but no diagnosis was made after a new MRI was reported as 'normal degenerative changes'.

DISCUSSION

Summary of findings

This study establishes an objective definition of spinal cord compression and found a high frequency of ASCC, increasing in frequency with age. Multiparametric quantitative MRI provided multiple lines of evidence suggesting that ASCC involves a mild degree of spinal cord tissue injury. Significant differences were found with five MRI metrics (rostral, MCL and caudal T2*WI WM/GM, rostral MTR and MCL FA), with T2*WI WM/GM and MTR results suggesting that demyelination is the predominant pathophysiological mechanism in these subjects.[12 13 19] The finding of decreased MCL FA confirms two previous reports,[18 20] and may be indicative of axonal injury

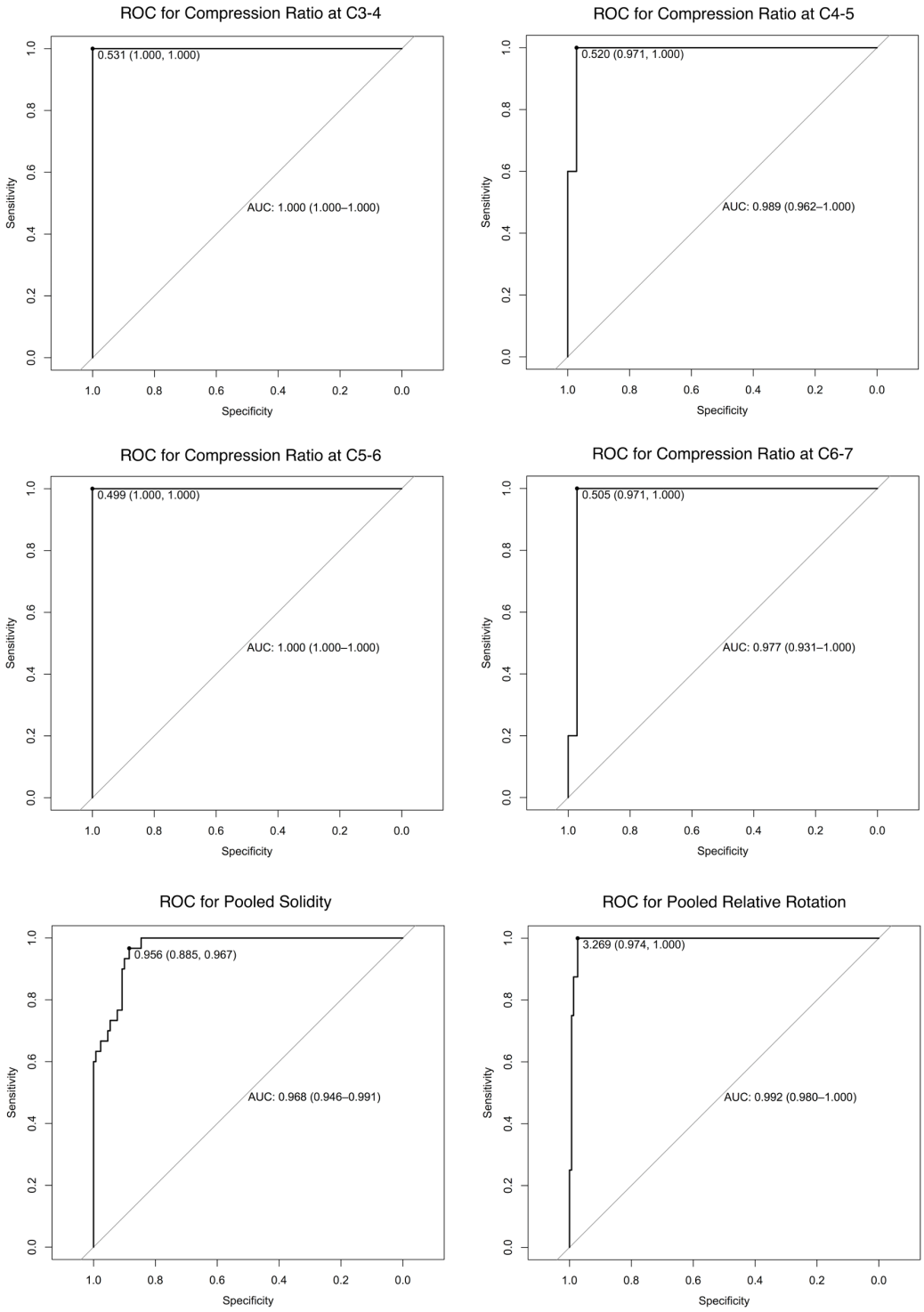

Figure 2 Receiver operating characteristic (ROC) curves for diagnosis of spinal cord compression using automated morphometric analysis. The results of automated shape analysis to diagnose spinal cord compression were compared against consensus ratings and ROC curves were plotted. The optimal threshold (maximising Youden's Index) is displayed, along with the sensitivity and specificity at that level. 95% CIs for area under the curve (AUC) are calculated using the Delong method.

but could alternatively be related to demyelination.[21] However, this result could also be artefactual, as DTI metrics can be biased in the compressed spinal cord by increased susceptibility artefact,[12 21] and thus it was reassuring that MRI measures also showed changes away from the compressed region. Furthermore, the study by Lindberg *et al*[20] included only five ASCC subjects, who showed functional deficits, while the Kerkovský *et al*[18] study included subjects with radiculopathy, which can localise within the spinal cord GM (ie, myeloradiculopathy). In contrast, our cohort was carefully screened to ensure the absence of neurological symptoms and signs. Recently, a larger study was completed with 92 ASCC and 71 uncompressed subjects, but DTI differences between these

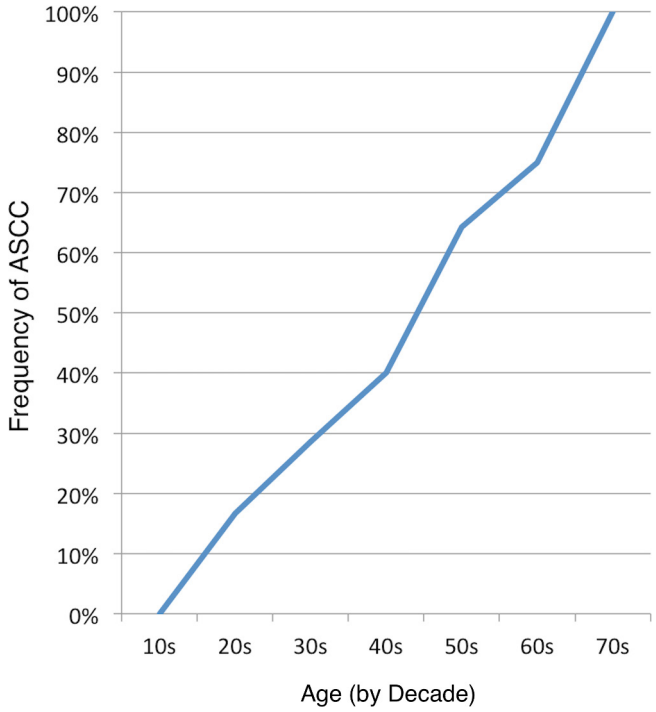

Figure 3 Frequency of ASCC by decade. The frequency of ASCC is plotted against decade of life, with data for each decade provided in parentheses. ASCC, asymptomatic spinal cord compression.

groups were not reported.[22] Our finding that rostral CSA was significantly greater among ASCC subjects suggests that atrophy does not occur in this condition, but rather, having a larger spinal cord appears to be a predisposing factor for compression, in keeping with a prior report that investigated spinal canal occupation ratio.[7] MCL CSA was also (non-significantly) larger in uncompressed subjects, but the ratio of MCL to rostral CSA showed a trend towards being decreased in ASCC, indicating that the mild compression observed in ASCC subjects has only a minor effect on CSA, and normalisation by rostral values helps to mitigate the high intersubject variability of this measure.[7 14] Although the groups with and without cord compression differed significantly in age and weight, all MRI metrics were corrected for age and none showed significant variation with weight. In fact, MTR and FA have previously been shown to vary with age,[11 14] but these relationships became non-significant when compression was included in the analysis, confirming a recent DTI study,[22] and suggesting that earlier studies may have overestimated the effect of age.[14 23 24] Spinal cord compression

Table 4 Comparison of metric ratios

MCL: rostral ratio	Uncompressed (n=20)	Compressed (n=20)	P values
CSA	1.050±0.060	1.003±0.106	0.09*
FA	0.917±0.054	0.878±0.056	0.06*
MTR	0.954±0.042	0.960±0.033	0.56
T2*WI WM/GM	1.005±0.029	1.001±0.025	0.67

Ratios were calculated by dividing MCL metric values by rostral values.
*Denotes significance (p<0.05).
CSA, cross-sectional area; DCM, degenerative cervical myelopathy; FA, fractional anisotropy; MCL, maximally compressed level; MTR, magnetisation transfer ratio; T2*WI WM/GM, T2*-weighted imaging white to grey matter.

Table 3 Comparison of normalised quantitative MRI metrics

Region	MRI metric	Uncompressed (n=20)	Compressed (n=20)	P values	Direction matches DCM
Rostral (C1–C3)	CSA	75.4±4.7	81.7±9.6	0.02*	N
	FA	0.731±0.031	0.720±0.037	0.48	Y
	MTR	53.6±3.0	51.9±1.8	0.046*	Y
	T2*WI WM/GM	0.838±0.029	0.863±0.031	0.03*	Y
Mid (MCL or C4–5)	CSA	79.2±7.7	81.9±12.8	0.34	N
	FA	0.670±0.044	0.631±0.043	0.04*	Y
	MTR	51.1±3.3	49.8±2.4	0.35	Y
	T2*WI WM/GM	0.842±0.019	0.864±0.026	0.005*	Y
Caudal (C6–C7)	FA	0.616±0.046	0.595±0.051	0.24	Y
	T2*WI WM/GM	0.845±0.037	0.881±0.050	0.01*	Y
Composite Score		0±1	−0.984±1.259	0.002*	Y

Normalised MRI metrics were compared between subjects with and without cord compression. A composite z score was used as an overall measure of tissue injury. Data extracted at the MCL were converted to z scores to normalise for rostrocaudal variations prior to comparison and then converted back to values at C4–5 for convenience of interpretation. The direction of differences (increases/decreases) in compressed versus uncompressed subjects was compared with previous findings in DCM versus healthy patients. Caudal CSA and MTR were not analysed because they did not show significant results in our prior DCM study.[15]
*Denotes significance (p<0.05).
CSA, cross-sectional area; DCM, degenerative cervical myelopathy; FA, fractional anisotropy; MCL, maximally compressed level; MTR, magnetisation transfer ratio; T2*WI WM/GM, T2*-weighted imaging white to grey matter.

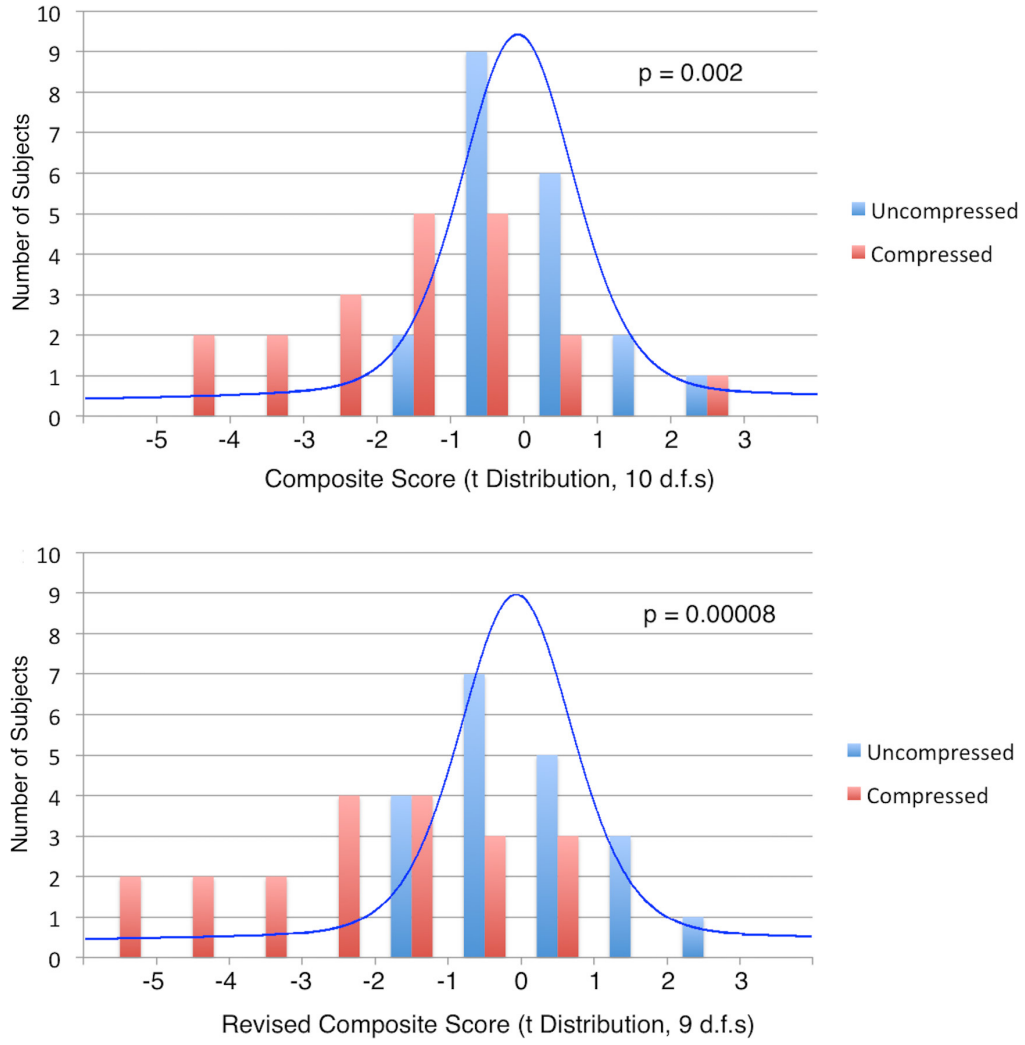

Figure 4 Distributions of composite scores. Top: histograms (bars) of composite scores (average of the z scores of 10 MRI metrics) are displayed for subjects with asymptomatic spinal cord compression (ASCC) (red) and no cord compression (blue). The expected distribution of results based on the null hypothesis (t-distribution with 10 df) is superimposed. Six ASCC subjects had abnormally low composite score ($t_{10} \leq 2.23$) and group differences were significant (Wilcoxon signed-rank test: p=0.002). Bottom: the same plot is displayed for a revised composite score that replaces rostral and maximally compressed levels cross-sectional area (CSA) measures with CSA ratio, and the corresponding t-distribution with 9 df. Nine ASCC subjects had abnormal scores ($t_9 \leq 2.26$) and stronger group differences were found (p=0.00008).

was primarily anterior in all subjects, and this appeared to preferentially cause injury to the ventral columns, as measured by reduced FA and MTR. T2*WI WM/GM demonstrated conflicting results with significant changes in lateral and dorsal columns and no significant effect in the ventral columns; we suspect that this is attributable to ventral artefacts on T2*WI, including chemical shift at the CSF-cord interface and blooming artefact from prominent anterior veins, but histopathological correlation is required. The grey matter did not show significant differences for FA or MTR, which is likely a limitation of these metrics as they are better at detecting white matter pathology.[12] Follow-up clinical data showed development of clinical myelopathy in 10% of subjects, similar to a prior report,[10] indicating that ASCC is a meaningful preclinical condition.

Our results highlight the value of multiparametric MRI and multivariate analysis; the combination of multiple tissue injury measures into a composite score is analogous (although not statistically equivalent) to taking n measurements of the same underlying value, which reduces the SE by $1/\sqrt{n}$. This is based on the assumption that the MRI measures are covariant, measuring the common entity of tissue injury. The revised composite score showed abnormal results in nine ASCC subjects, and logistic regression suggested that the majority of subjects with ASCC experience tissue injury. However, such data-driven analysis may suffer from overfitting and must be interpreted with caution. In fact, without histopathological studies, the ground truth is unknown regarding microstructural changes that occur in ASCC, and to our knowledge no cadaver studies have investigated this topic.

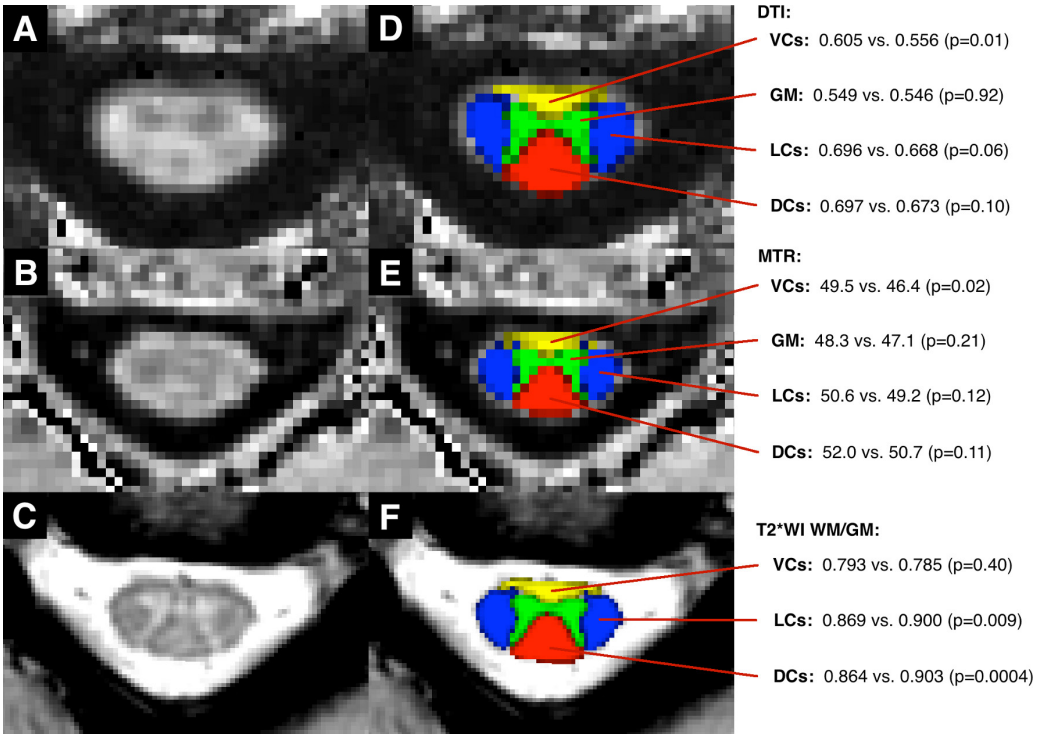

Figure 5 Quantitative MRI metrics by anatomical structure. Images include a FA map (A), a MTR map (B) and a T2*-weighted image (C) of C3–4 in an uncompressed subject. Panels (D–F) The SCT probabilistic maps of the VCs (yellow), LCs (blue), DCs (red) and GM (green) overlaid. DCs, dorsal columns; DTI, diffusion tensor imaging; FA, fractional anisotropy; GM, grey matter; LCs, lateral columns; MTR, magnetisation transfer ratio; SCT, Spinal Cord Toolbox; VCs, ventral columns, T2*WI WM/GM, T2*-weighted imaging white to grey matter.

Overall, the results support our hypothesis at a group level, suggesting that spinal cord tissue injury begins in subjects with mild compression prior to the manifestation of clinical symptoms or signs. This offers the intriguing possibility of presymptomatic diagnosis in this condition and others, with far-reaching potential clinical applications. However, further investigation in a larger cohort of subjects with long-term follow-up is needed to confirm the findings of this study and to better characterise the prevalence of ASCC, relationship with age, rate of symptomatic myelopathy development and specific prognostic factors.

An objective definition of spinal cord compression

The high frequencies of ASCC in our data are similar to the range of 51.5%–66.2% (for age 40–80) reported by Kovalova *et al*,[8] but far higher than earlier reports of 8%–26%.[3–7] These differences are primarily due to vague and subjective definitions of spinal cord compression in prior studies, which used the terms impingement, encroachment and compression without strict criteria.[3–7] Kerkovský *et al* provided a more precise definition of spinal cord compression: a concave defect adjacent to a bulging disc or osteophyte and/or CR <0.4[18]; however, their threshold for CR was very low, at 4.5 SDs below the mean (based on our normative data at C5–6) and did not account for normal variations of CR across levels. Furthermore, the error associated with manual CR measurement has not been characterised, and visual assessment of concavity is subjective. Kovalova *et al* provided detailed descriptions of indentation, flattening and circumferential compression, but did not establish quantitative criteria.[8] Instead, we use automated analysis to reduce bias and define spinal cord compression as deviation from normal spinal cord morphology in three quantitative parameters that reflect flattening, indentation and torsion (due to lateral bulging discs). This approach identified four levels of subtle compression missed by two expert raters and achieved excellent diagnostic accuracy. 2D PCA readily detects the transverse axis of the spinal cord, allowing calculation of CR and relative rotation, while indentation is robustly calculated using convex hulls. Several additional shape parameters are also under investigation including asymmetry indices to detect lateral compression and relative CSA to detect circumferential compression, but these were not necessary in this cohort. Automatic analysis is fast and straightforward using the free open-source SCT,[16] and the only manual step is reviewing and editing the segmentation. Our results define normative data for each shape parameter across cervical intervertebral levels, and ROC analysis identified diagnostic thresholds that were close to 2 SDs from the mean of each metric. Many of our ASCC cases showed CSF intervening between the compressive process (eg, disc osteophyte complex) and the ventral spinal cord surface, as the spinal cord shifts posteriorly when the subject is supine. This indicates that the cord

deformity is observed in the absence of visible compression, suggesting that shape analysis can detect dynamic spinal cord compression, which has previously only been possible with flexion/extension MRI.[25]

Contemplating the definition of myelopathy

Myelopathy is typically defined as 'a disease or disorder of the spinal cord', and our results suggest that individuals with ASCC may meet this description. In contrast, clinicians have historically favoured functional criteria: the presence of neurological symptoms and signs that localise to the spinal cord.[26] This clinical definition most likely originated due to the lack of diagnostic investigations that can accurately detect early pathological changes within the cord. It appears that symptoms and signs of myelopathy only emerge once a considerable degree of tissue injury occurs, and we suspect that homoeostatic mechanisms of neuroplasticity and behavioural adaptation act to mask early changes. Technological advances have led to the emergence of in vivo diagnostic tools, including MRI, that have the potential to surpass clinical assessments by taking direct measurements from the spinal cord. Similar progress has been made in electrophysiology with the development of contact heat evoked potentials (CHEPs),[27] which appear to be more sensitive than motor and sensory evoked potentials for myelopathy.[18] As these tools become more sophisticated and refined, they will allow progressively earlier detection of tissue injury in this condition, in which the ground truth likely constitutes a continuum between normal and abnormal without a clear division, similar to degenerative processes in the ageing brain.

Clinical implications

The radiological findings of mild spinal cord indentation and flattening are of unknown significance and in the authors' experience these are frequently dismissed (as seen in one subject that progressed to symptomatic myelopathy). However, the results of this study suggest that ASCC involves degradation of the tissue microstructure, likely representing a preclinical state akin to the prediabetic diagnosis of insulin resistance. Furthermore, these patients appear to be at increased risk for progression to clinical myelopathy, consistent with a prior study found that 8% of individuals with ASCC develop symptomatic myelopathy at 1 year and 22.6% at 4 years, with risk factors including presence of radiculopathy, T2WI hyperintensity or prolonged conduction on electrophysiology studies.[10] Thus, individuals with ASCC should be educated about myelopathy symptoms, and further research is warranted to determine a potential role for MRI screening and longitudinal clinical follow-up. Unfortunately, patients often ignore early neurological symptoms, as was evident in two excluded subjects with evidence of mild DCM, of which they were not aware. Furthermore, additional efforts are needed to educate primary care clinicians so that prompt diagnosis of DCM can be made before debilitating symptoms have developed, at which point surgical treatment rarely restores normal ambulation and hand function. Earlier diagnosis of DCM would allow earlier treatment, and surgery is associated with reduced morbidity in all severity categories including mild DCM.[28] Preliminary results suggest that serial quantitative MRI assessments may also be helpful in detecting progression of tissue injury,[29] and long-term clinical and quantitative MRI monitoring of this cohort of ASCC subjects is planned. Quantitative MRI may also hold potential for earlier diagnosis of other spinal conditions, which share pathophysiological mechanisms of demyelination, axonal injury, gliosis and atrophy.[13]

Limitations

The statistical methods used in this study (including normalisation, age correction, regression) are somewhat complex and involve several assumptions that require validation (eg, normality). Statistical correction for multiple comparisons was not performed due to the exploratory nature of this study, but should be incorporated into the design of future confirmatory studies. The sample size of 40 subjects is too small to accurately estimate prevalence and the rate of myelopathy development, and larger confirmatory studies are required. Our normalisation approach for age and other subject characteristics may be inaccurate, and ideally groups would be matched for these variables (although this is difficult because ASCC is age related and its presence was unknown at time of recruitment). Quantitative shape analysis is dependent on an accurate spinal cord segmentation, and manual editing of segmentations was necessary in most subjects. Automatic segmentation of the compressed spinal cord is challenging due to anatomical distortion and reduced contrast with surrounding tissues, and alternative approaches are under investigation. Shape analysis would be enhanced by using an optimised high-resolution T2WI acquisition, but our T2WI had only moderate resolution and frequently showed motion artefacts. The use of convenience sampling may constitute selection bias, as individuals who have concerns of spinal pathology may be more likely to volunteer for an MRI study. Follow-up physical examinations were only performed for subjects that reported new symptoms, which could constitute information bias. The presence of metallic hardware (eg, dental) was not grounds for exclusion, and this could bias MRI results but was not factored into the analysis. Consensus ratings for the presence of compression were used as a reference but their validity was not investigated.

CONCLUSIONS

ASCC appears to be a common age-related condition that can be accurately and objectively diagnosed with automated analysis of spinal cord morphology. Furthermore, ASCC appears to involve similar macrostructural and microstructural changes as symptomatic DCM, and this condition may confer an increased risk of symptomatic myelopathy development. These results require further validation, but they suggest a potential role for educating and monitoring ASCC subjects for symptoms and signs of myelopathy, while offering the possibility of

presymptomatic diagnosis and treatment of other spinal pathologies.

Contributors All authors provided final approval of this manuscript to be published. All authors agreed to be accountable for all aspects of the work. ARM: primary contributor to study conception, design, clinical examinations of subjects, MRI data collection, image analysis, statistical analysis and manuscript writing. This study was part of ARM's PhD thesis work at University of Toronto. BDL and JC-A: contributed to study design, MRI data collection, image analysis, spinal cord shape analysis, statistical analysis and manuscript editing. DWC, APC, DJM and HG: contributed to study design, statistical analysis and manuscript editing. AN: contributed to study design, clinical examinations, MRI data collection, image analysis, statistical analysis and manuscript editing. JRW: contributed to statistical analysis and manuscript editing. LT: contributed to MRI data collection, statistical analysis and manuscript editing. MGF: senior author and PhD supervisor to ARM. Contributed to study conception, design, clinical examinations, statistical analysis and manuscript editing.

Funding This research received funding from Rick Hansen Institute, grant number RHI-2014-12, as part of the Riluzole in Spinal Cord Injury Study (RISCIS), which is also supported by AOSpine North America, AOSpine International SCI Knowledge Forum and the North American Clinical Trials Network (NACTN) of the Christopher and Dana Reeve Foundation. This research also received support from the Dezwirek Foundation, the Sherman Clinical Research Unit and the Gerald and Tootsie Halbert Chair in Spinal Cord Research. ARM received postdoctoral fellowship support from Canadian Institutes of Health Research, grant number 201511MFE-359116-246227.

Competing interests None declared.

Patient consent Detail has been removed from this case description/these case descriptions to ensure anonymity. The editors and reviewers have seen the detailed information available and are satisfied that the information backs up the case the authors are making.

Ethics approval This study received institutional approval from University Health Network (UHN, Toronto, Ontario, Canada)

Provenance and peer review Not commissioned; externally peer reviewed.

Data sharing statement Extra data can be accessed via the Dryad data repository at http://datadryad.org/ with the doi:10.5061/dryad.kk653rs

REFERENCES

1. Nouri A, Tetreault L, Singh A, *et al*. Degenerative cervical myelopathy: epidemiology, genetics, and pathogenesis. *Spine* 2015;40:E675–93.
2. Kalsi-Ryan S, Karadimas SK, Fehlings MG. Cervical spondylotic myelopathy: the clinical phenomenon and the current pathobiology of an increasingly prevalent and devastating disorder. *Neuroscientist* 2013;19:409–21.
3. Teresi LM, Lufkin RB, Reicher MA, *et al*. Asymptomatic degenerative disk disease and spondylosis of the cervical spine: MR imaging. *Radiology* 1987;164:83–8.
4. Boden SD, McCowin PR, Davis DO, *et al*. Abnormal magnetic-resonance scans of the cervical spine in asymptomatic subjects. A prospective investigation. *J Bone Joint Surg Am* 1990;72:1178–84.
5. Matsumoto M, Fujimura Y, Suzuki N, *et al*. MRI of cervical intervertebral discs in asymptomatic subjects. *J Bone Joint Surg Br* 1998;80:19–24.
6. Lee MJ, Cassinelli EH, Riew KD. Prevalence of cervical spine stenosis. Anatomic study in cadavers. *J Bone Joint Surg Am* 2007;89:376–80.
7. Kato F, Yukawa Y, Suda K, *et al*. Normal morphology, age-related changes and abnormal findings of the cervical spine. Part II: magnetic resonance imaging of over 1,200 asymptomatic subjects. *Eur Spine J* 2012;21:1499–507.
8. Kovalova I, Kerkovsky M, Kadanka Z, *et al*. Prevalence and imaging characteristics of nonmyelopathic and myelopathic spondylotic cervical cord compression. *Spine* 2016;41:1908–16.
9. Bartlett RJ, Hill CA, Rigby AS, *et al*. MRI of the cervical spine with neck extension: is it useful? *Br J Radiol* 2012;85:1044–51.
10. Bednarik J, Kadanka Z, Dusek L, *et al*. Presymptomatic spondylotic cervical myelopathy: an updated predictive model. *Eur Spine J* 2008;17:421–31.
11. Martin AR, Aleksanderek I, Cohen-Adad J, *et al*. Translating state-of-the-art spinal cord MRI techniques to clinical use: A systematic review of clinical studies utilizing DTI, MT, MWF, MRS, and fMRI. *Neuroimage Clin* 2016;10:192–238.
12. Stroman PW, Wheeler-Kingshott C, Bacon M, *et al*. The current state-of-the-art of spinal cord imaging: methods. *Neuroimage* 2014;84:1070–81.
13. Wheeler-Kingshott CA, Stroman PW, Schwab JM, *et al*. The current state-of-the-art of spinal cord imaging: applications. *Neuroimage* 2014;84:1082–93.
14. Martin AR, De Leener B, Cohen-Adad J, *et al*. Clinically feasible microstructural MRI to quantify cervical spinal cord tissue injury using DTI, MT, and T2*-weighted imaging: assessment of normative data and reliability. *AJNR Am J Neuroradiol* 2017;38:1257–65.
15. Martin AR, De Leener B, Cohen-Adad J, *et al*. A novel MRI biomarker of spinal cord white matter injury: T2*-weighted white matter to grey matter signal intensity ratio. *AJNR*. In Press. 2017.
16. De Leener B, Lévy S, Dupont SM, *et al*. SCT: spinal cord toolbox, an open-source software for processing spinal cord MRI data. *Neuroimage* 2017;145:24–43.
17. Kameyama T, Hashizume Y, Ando T, *et al*. Morphometry of the normal cadaveric cervical spinal cord. *Spine* 1994;19:2077–81.
18. Kerkovský M, Bednarík J, Dušek L, *et al*. Magnetic resonance diffusion tensor imaging in patients with cervical spondylotic spinal cord compression: correlations between clinical and electrophysiological findings. *Spine* 2012;37:48–56.
19. Cohen-Adad J. What can we learn from T2* maps of the cortex? *Neuroimage* 2014;93(Pt 2):189–200.
20. Lindberg PG, Sanchez K, Ozcan F, *et al*. Correlation of force control with regional spinal DTI in patients with cervical spondylosis without signs of spinal cord injury on conventional MRI. *Eur Radiol* 2016;26:733–42.
21. Cohen-Adad J, El Mendili MM, Lehéricy S, *et al*. Demyelination and degeneration in the injured human spinal cord detected with diffusion and magnetization transfer MRI. *Neuroimage* 2011;55:1024–33.
22. Keřkovský M, Bednařík J, Jurová B, *et al*. Spinal cord MR diffusion properties in patients with degenerative cervical cord compression. *J Neuroimaging* 2017;27:149–57.
23. Mamata H, Jolesz FA, Maier SE. Apparent diffusion coefficient and fractional anisotropy in spinal cord: age and cervical spondylosis-related changes. *J Magn Reson Imaging* 2005;22:38–43.
24. Taso M, Girard OM, Duhamel G, *et al*. Tract-specific and age-related variations of the spinal cord microstructure: a multi-parametric MRI study using diffusion tensor imaging (DTI) and inhomogeneous magnetization transfer (ihMT). *NMR Biomed* 2016;29:817–32.
25. Nouri A, Martin AR, Mikulis D, *et al*. Magnetic resonance imaging assessment of degenerative cervical myelopathy: a review of structural changes and measurement techniques. *Neurosurg Focus* 2016;40:E5.
26. Seidenwurm DJ. Myelopathy. *AJNR Am J Neuroradiol* 2008;29:1032–4.
27. Jutzeler CR, Ulrich A, Huber B, *et al*. Improved diagnosis of cervical spondylotic myelopathy with contact heat evoked potentials. *J Neurotrauma* 2017;34:2045–53.
28. Fehlings MG, Wilson JR, Kopjar B, *et al*. Efficacy and safety of surgical decompression in patients with cervical spondylotic myelopathy: results of the AOSpine North America prospective multi-center study. *J Bone Joint Surg Am* 2013;95:1651–8.
29. Martin AR, De Leener B, Cohen-Adad J, *et al*. *Toward clinical translation of quantitative spinal cord MRI: serial monitoring to identify disease progression in patients with degenerative cervical myelopathy*. Honolulu, Hawaii, USA: International Society for Magnetic Resonance in Medicine, 2017.